

Radar Waveform Optimization for Colored Noise Mitigation

Jameson S. Bergin, Paul M. Techau, and John E. Don Carlos, Information Systems Laboratories, Inc.
Joseph R. Guerri, Defense Advanced Research Projects Agency

Key Words: radar, transmitter, optimization, interference, mitigation

SUMMARY AND CONCLUSIONS

Waveform optimization is a technique that can be used to adjust any or all of the radar transmitter degrees of freedom (DoFs) based on observations of a dynamic environment caused by intentional and/or unintentional interference sources. These DoFs include but are not limited to pulse shape, pulse repetition frequency (PRF), bandwidth, and operating frequency. Waveform optimization techniques can potentially provide an additional tool to improve radar system performance in severe operating environments. This paper addresses the use of waveform optimization in radio frequency interference (RFI) environments, particularly in the situation where the RFI signal is partial band or is scattered into the radar receiver main beam by terrain (hot clutter).

1.0 INTRODUCTION

Waveform optimization is a technique that can be used to adjust any or all of the radar transmitter degrees of freedom (DoFs) based on observations of a dynamic environment caused by intentional and/or unintentional interference sources. These DoFs include but are not limited to pulse shape, pulse repetition frequency (PRF), bandwidth, and operating frequency. While adaptivity on receive has been exploited for quite some time [1-3] waveform optimization provides the promise of the development of a fully adaptive radar. Recent work has resulted in various techniques for applying this optimization [4-6]. Waveform optimization techniques can potentially provide an additional tool to improve system performance in severe operating environments.

This paper addresses the use of waveform optimization in radio frequency interference (RFI) environments, particularly in the situation where the RFI signal is partial band or is scattered into the radar receiver main beam by terrain (hot clutter). There can be significant coverage losses due to terrain-scattered interference. For finite aperture the only solution may be to “burn through” which will impact the radar time line. Waveform optimization can potentially provide an alternative to this by emphasizing (matching) to the target and de-emphasizing (anti-matching) to the interference.

Section 2 summarizes the application of waveform optimization theory to RFI mitigation and develops a bound on the

achievable gain of the optimal waveform in terms of the eigenvalues of the covariance matrix of the RFI signal. Section 3 summarizes the waveform optimization algorithms employed in the study. Section 4 provides analysis of the performance of waveform optimization techniques in the presence of band-limited white-noise RFI and terrain-scattered interference. Summary and conclusions are provided in Section 5.

2.0 SUMMARY OF THEORY AND PERFORMANCE BOUND

We begin by considering the optimum receiver configuration for a signal corrupted by wide-sense stationary (w.s.s) additive colored noise (ACN) and follow the development of [4-6]. This configuration is shown in Figure 1. It is well known that the signal-to-interference-plus-noise ratio (SINR) is maximized when the received signal $x(t)$ is first whitened to cancel the ACN and then detected using a filter matched to the ‘whitened’ waveform [8] i.e.,

$$s_w(t) = s(t) * h_w(t); h_{MF}(t) = [s_w(t - T)]^*,$$

where $*$ denotes linear convolution and superscript $*$ denotes the complex conjugate. Thus the output is then

$$y(t) = s_T(t) * h_R(t);$$

where $h_R(t) = h_w(t) * h_{MF}(t)$.

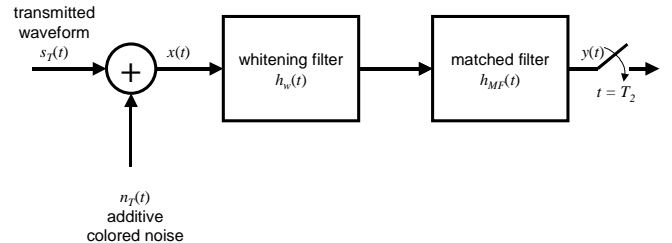


Fig. 1. Optimal receiver configuration for detecting a signal in additive colored noise.

Given this receiver structure, our task is now to exploit the degrees of freedom (DoFs) available in the transmit waveform to maximize the SINR. Again, following [4-6], we first consider the SINR of the optimally filtered received signal:

$$\text{SINR}_0 = \frac{1}{2} \int_{T_1}^{T_2} |s_w(t)|^2 dt$$

where σ_w^2 is the power spectral density of the whitened ACN and T_1 and T_2 are the limits of the observation interval. To maximize the SINR, we must maximize the energy in the whitened signal over all possible transmit waveforms. Thus we wish to solve:

Presented at the 2005 IEEE Radar Conference, Alexandria, VA, 9-12 May, 2005.

This work was sponsored under Air Force Contract F30602-02-C-0005.

Approved for Public Release. Distribution Unlimited.

Report Documentation Page				Form Approved OMB No. 0704-0188	
Public reporting burden for the collection of information is estimated to average 1 hour per response, including the time for reviewing instructions, searching existing data sources, gathering and maintaining the data needed, and completing and reviewing the collection of information. Send comments regarding this burden estimate or any other aspect of this collection of information, including suggestions for reducing this burden, to Washington Headquarters Services, Directorate for Information Operations and Reports, 1215 Jefferson Davis Highway, Suite 1204, Arlington VA 22202-4302. Respondents should be aware that notwithstanding any other provision of law, no person shall be subject to a penalty for failing to comply with a collection of information if it does not display a currently valid OMB control number.					
1. REPORT DATE 01 MAY 2005		2. REPORT TYPE N/A		3. DATES COVERED -	
4. TITLE AND SUBTITLE Radar Waveform Optimization for Colored Noise Mitigation				5a. CONTRACT NUMBER	
				5b. GRANT NUMBER	
				5c. PROGRAM ELEMENT NUMBER	
6. AUTHOR(S)				5d. PROJECT NUMBER	
				5e. TASK NUMBER	
				5f. WORK UNIT NUMBER	
7. PERFORMING ORGANIZATION NAME(S) AND ADDRESS(ES) Information Systems Laboratories, Inc.				8. PERFORMING ORGANIZATION REPORT NUMBER	
9. SPONSORING/MONITORING AGENCY NAME(S) AND ADDRESS(ES)				10. SPONSOR/MONITOR'S ACRONYM(S)	
				11. SPONSOR/MONITOR'S REPORT NUMBER(S)	
12. DISTRIBUTION/AVAILABILITY STATEMENT Approved for public release, distribution unlimited					
13. SUPPLEMENTARY NOTES See also ADM002017. Proceedings of the 2005 IEEE International Radar Conference Record Held in Arlington, Virginia on May 9-12, 2005. U.S. Government or Federal Purpose Rights License., The original document contains color images.					
14. ABSTRACT					
15. SUBJECT TERMS					
16. SECURITY CLASSIFICATION OF:			17. LIMITATION OF ABSTRACT UU	18. NUMBER OF PAGES 6	19a. NAME OF RESPONSIBLE PERSON
a. REPORT unclassified	b. ABSTRACT unclassified	c. THIS PAGE unclassified			

$$\begin{aligned} \max_{s_T(t)} \int_{T_1}^{T_2} |s_w(t)|^2 dt &\Rightarrow \max_{s_T(t)} \int_{T_1}^{T_2} |s_T(t) * h_w(t)|^2 dt \Rightarrow \\ \max_{s_T(t)} \int_{T_1}^{T_2} \left(\int_0^T s_T(\tau_1) h_w(t - \tau_1) d\tau_1 \right) &\left(\int_0^T s_T(\tau_2) h_w(t - \tau_2) d\tau_2 \right)^* dt \end{aligned}$$

and we have made the assumption that the transmit waveform is of finite duration over the interval of $[0, T]$. Rearranging terms and changing the order of integration yields:

$$\begin{aligned} \max_{s_T(t)} \int_0^T s_T(\tau_1) \int_0^T s_T(\tau_2) h_w(t - \tau_1) \times \\ \left(\int_{T_1}^{T_2} h_w^*(t - \tau_1) h_w(t - \tau_2) dt \right)^* d\tau_2 d\tau_1 \end{aligned}$$

where the last term is the conjugate of the kernel (which bears a resemblance to the autocorrelation) function of $h_w(t)$ that we denote $K(\tau_1, \tau_2)$. If we apply Schwarz's inequality, we find the optimal waveform $s_0(t)$ to be the solution of

$$\lambda_{max} s_0(\tau_1) = \int_0^T s_0(\tau_2) K(\tau_1, \tau_2) d\tau_2$$

that is, the optimal waveform is an eigenfunction associated with the maximum eigenvalue of the kernel $K(\tau_1, \tau_2)$.

If we consider a practical implementation using discrete-time signals, we have the receiver structure shown in Figure 2. Now the optimum SINR is given by

$$\text{SINR}_0 = \frac{\|s_w\|^2}{\sigma_w^2} = \frac{\|H_w^H s_T\|^2}{\sigma_w^2} = \frac{s_T^H H_w H_w^H s_T}{\sigma_w^2}$$

where H denotes the Hermitian transpose, $\|\cdot\|$ is the L-2 norm, and again this quantity can be maximized by appropriate selection of s_T . This will be the eigenvector associated with the maximum eigenvalue of $H_w H_w^H$. It is well-known that the whitening filter to cancel the ACN \mathbf{n} is $\mathbf{H}_w = \mathbf{R}_n^{-1/2}$ where $\mathbf{R}_n = E[\mathbf{n}\mathbf{n}^H]$ and $E[\cdot]$ is the expectation operator. Thus \mathbf{R}_n is a Toeplitz matrix with the appropriate autocovariance lags along each diagonal. (This can be verified by considering $E[(\{\mathbf{R}_n^{-1/2}\}^H \mathbf{n})(\{\mathbf{R}_n^{-1/2}\}^H \mathbf{n})^H]$). Thus the optimal transmit waveform is $\mathbf{s}_0 = \mathbf{u}_{min}$ where \mathbf{u}_{min} is the eigenvector associated with the minimum eigenvalue λ_{min} of \mathbf{R}_n .

We note that the output of the receiver of Figure 1 can be written as

$$y = \mathbf{h}_{MF}^H \mathbf{H}_w^H \mathbf{x} = \mathbf{s}_T^H \mathbf{H}_w \mathbf{H}_w^H \mathbf{x}.$$

When the optimal waveform is used, $\mathbf{s}_T = \mathbf{u}_{min}$. Since $\mathbf{R}_n = (\mathbf{H}_w \mathbf{H}_w^H)^{-1}$ can be written as $\mathbf{U}\Lambda\mathbf{U}^H$, where \mathbf{U} is a matrix whose columns are the eigenvectors of \mathbf{R}_n and Λ is a matrix whose diagonal elements are the eigenvalues of \mathbf{R}_n , we can write

$$y = \mathbf{u}_{min}^H \mathbf{U} \Lambda^{-1} \mathbf{U}^H \mathbf{x} = \lambda_{min}^{-1} \mathbf{u}_{min}^H \mathbf{x}.$$

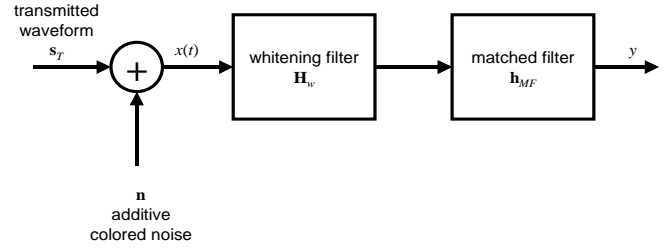


Fig. 2. Discrete-time form optimal receiver configuration for detecting a signal in additive colored noise. Vectors of the various time series are indicated by \mathbf{s}_T , \mathbf{n} , \mathbf{x} , and \mathbf{h}_{MF} while \mathbf{H}_w represents a matrix transformation.

Thus when the optimal waveform is used, the whitening filter stage of Figure 1 can be eliminated.

If we define λ_{min} and λ_{max} as the minimum and maximum eigenvalues of \mathbf{R}_n , respectively, then the minimum and maximum eigenvalues of \mathbf{R}_n^{-1} are $1/\lambda_{max}$ and $1/\lambda_{min}$, respectively. We then see that the SINR is bounded as shown [7]:

$$\frac{\sigma_w^2}{\lambda_{max}} \leq \text{SINR}_0 \leq \frac{\sigma_w^2}{\lambda_{min}}.$$

This double sided inequality also leads to an upper bound on the achievable gain of the optimal waveform over any other arbitrary waveform. This is [7]:

$$g \leq \frac{\sigma_w^2 / \lambda_{min}}{\sigma_w^2 / \lambda_{max}} = \frac{\lambda_{max}}{\lambda_{min}} \quad (1)$$

where g is the relative gain between a radar that uses the optimal waveform and one that uses some other suboptimal waveform. Therefore, the achievable gain is characterized by the eigenvalue spread of the interference covariance matrix. It is interesting to note that when the radar observation interval is long the eigenvectors (eigenfunctions in the continuous-time case) become complex exponentials (see [8] p. 205) and the bound given in (1) can be expressed as the ratio of the maximum and minimum value of the interference power spectral density (PSD) over the system bandwidth. That is,

$$g \leq \frac{\max_f N(f)}{\min_f N(f)}$$

where $N(f)$ is the PSD of the interference signal.

3.0 ALGORITHMS

We consider three methods for calculating the transmit waveform based on the interference (temporal) covariance. 'Method 1' is to simply choose the eigenvector associated with the minimum eigenvalue of the interference covariance [4-6]. The rationale is to place the transmit energy into the dimension with the least amount of interference. In this case, since eigenvectors have a unity norm, the optimum waveform $\mathbf{s}_0 = \mathbf{u}_{min}$ is normalized to unit energy.

'Method 2' takes advantage of the rank-deficient nature of the interference of Figure 3 and uses the sum of all of the eigenvectors corresponding to eigenvectors at or below the noise

level, and then normalizing the result to unit energy. Thus we have:

$$\mathbf{s}_0 = \gamma \sum_{k=1}^{K'} \mathbf{u}_k \quad (2)$$

where $\mathbf{u}_k, k = 1 \dots K'$ are the ‘noise’ eigenvectors (i.e., the eigenvectors not associated with the ‘colored’ interference) and γ is chosen so the result has unit energy. This method adds flexibility for the optimum waveform to spread out over the entire fraction of the band not occupied by the interference.

‘Method 3’, which is similar to the approach taken in [9], recognizes that traditional waveforms have many desirable characteristics (constant modulus, ability to control range sidelobes in radar applications, etc.). Thus the objective is to find a set of weights α_k such that

$$\mathbf{s}_0 = \gamma \sum_{k=1}^{K'} \alpha_k \mathbf{u}_k$$

is ‘closest’ in a least-squares sense to some desired waveform. The constant γ again is chosen to normalize the waveform to unit energy. To obtain the desired result, we simply need to solve the equation:

$$\frac{\mathbf{s}_0}{\gamma} = \sum_{k=1}^{K'} \alpha_k \mathbf{u}_k = \mathbf{U}_{K'} \underline{\alpha} = \mathbf{s}_d \quad (3)$$

where $\mathbf{U}_{K'} = [\mathbf{u}_1 \mathbf{u}_2 \dots \mathbf{u}_{K'}]$; $\underline{\alpha} = [\alpha_1 \alpha_2 \dots \alpha_{K'}]^T$; and \mathbf{s}_d is a vector representation of the desired waveform (below we provide examples using a linear frequency modulated (LFM) waveform). To solve for $\underline{\alpha}$, we simply multiply the last two expressions of (3) by $\mathbf{U}_{K'}^H$ and exploit the unitary nature of $\mathbf{U}_{K'}$. Thus we find the result

$$\mathbf{s}_0 = \gamma \mathbf{U}_{K'} \mathbf{U}_{K'}^H \mathbf{s}_d. \quad (4)$$

4.0 SIMULATIONS

Each of the techniques discussed in Section 3 was analyzed in terms of SINR performance and ability to maintain desirable radar waveform characteristics such as constant modulus and low range sidelobes.

4.1. Band-Limited Interference

In the presence of interference that is white noise that has been band-limited, the performance gain will come principally from isolating the transmit energy into interference-free regions of the system band. Thus these gains will of course be greatest when the interference bandwidth is less than the system bandwidth. To examine this, we consider the scenario illustrated in the Figure 3, where the interference is shown to be some fraction of the system bandwidth. While we do not expect a difference in performance based on the location of the interference within the system band, we consider both the offset and centered cases shown to verify this assumption.

We first consider the case of a 1 MHz system bandwidth and a 100 kHz interference bandwidth. In Figure 4,

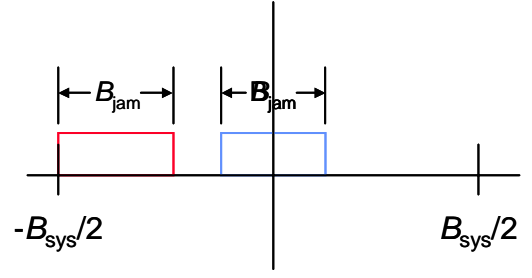


Fig. 3. Interference spectra vs. system bandwidth.

the spectra of the interference and the optimal waveform (Method 1) are shown for an offset case, along with the pulse-compressed (detected) waveform moduli as a function of time. The results for Method 2 for the same case are shown in Figure 5. Here we see a result similar to Method 1.

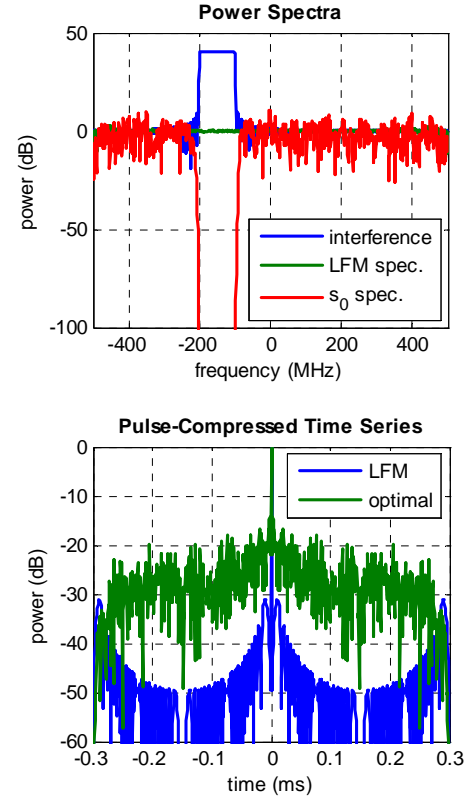


Fig. 4. Top: waveform spectra, Method 1 optimization. Bottom: corresponding time series.

This is in contrast with Method 3, for which results are shown in Figure 6. Here we see that the pulse-compressed output is much more well behaved and retains much of the range sidelobe characteristic of the LFM waveform.

A summary of SINR performance is shown in Figure 7. We consider gain in SINR relative to a LFM waveform. We see that none of the three methods attains the bound when the interference is a smaller fraction of the system bandwidth, although substantial gains do result. In these particular cases, large gains are possible as a result of concentrating all of the interference energy in the ‘clear’ part of the spectrum. (In other

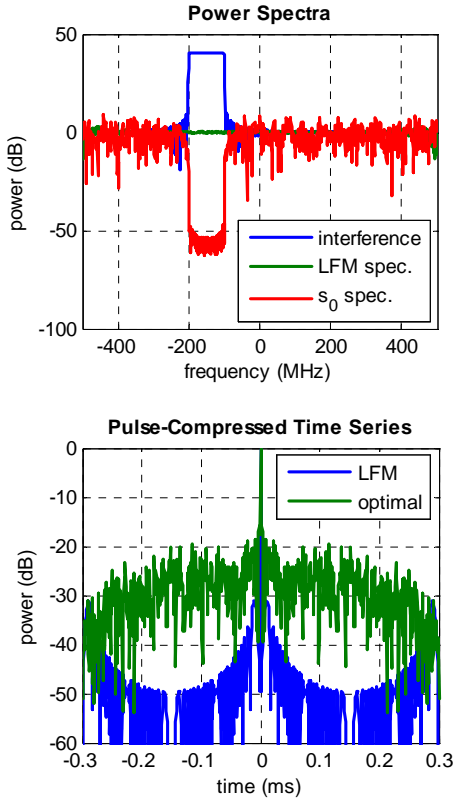


Fig. 5. Top: waveform spectra, Method 2 optimization. Bottom: corresponding time series.

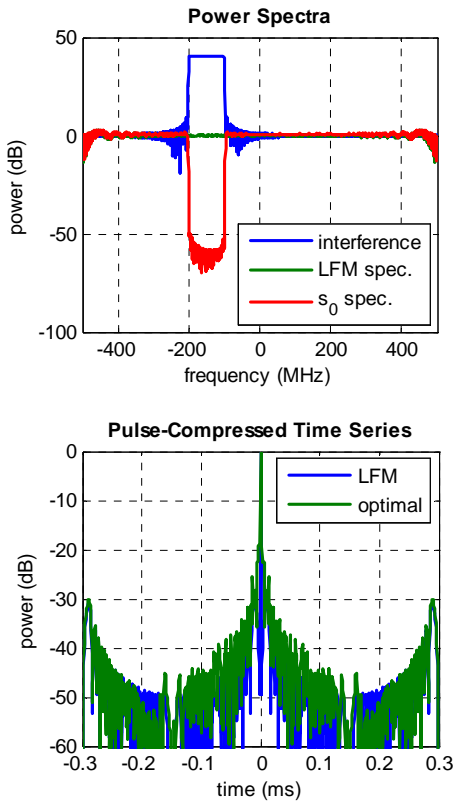


Fig. 6. Top: waveform spectra, Method 3 optimization. Bottom: corresponding time series.

scenarios, this may not be possible, and smaller gains may result.) Thus, considering the desirable sidelobe and modulus characteristics of Method 3, this would typically be the preferred method of the three described herein. Finally, we also note as expected that there is little SINR performance difference among the methods or between the ‘centered’ and ‘offset’ cases.

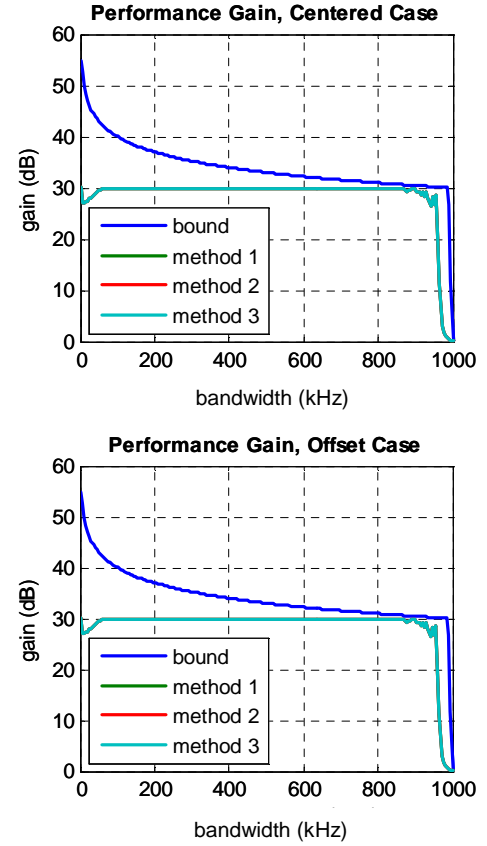


Fig. 7. SINR performance gain summary. Top: ‘centered’ case. Bottom: ‘offset’ case. Here, ‘gain’ denotes the potential/achieved gain in SINR relative to a LFM waveform.

We note that the performance gains shown herein are relative to the use of an LFM waveform without the use of the whitening filter of Figure 1. Future analyses will consider the impact of the whitening filter in combination with optimal waveforms.

4.2. Terrain-Scattered Interference

Terrain-scattered interference (TSI) [10-13] results when terrain-scattered signals from an interference source are scattered into the radar receiver main beam. Space-time adaptive signal processing can mitigate the interference but at a performance cost when radar clutter and TSI must be jointly mitigated.

Since the multiple delay (and Doppler-shifted) signals of the interference that comprise the TSI will be colored, the potential exists to optimize the radar transmit waveform to occupy temporal eigenspace where the interference is weak, thereby improving the radar signal-to-interference ratio without using space-time degrees of freedom. Even small improve-

ments can be significant in reducing burn-through requirements or interference rank. However, motion of the interference and/or receiver platform results in the interference being non-stationary [10, 11], thus latency becomes an issue.

The interference signal was assumed to be white covering the full radar bandwidth. The signal as received on a direct path is not colored, and if not spatially notched, diminishes the advantage of the optimized waveform. The radar adapts to the colored interference by estimating the temporal covariance matrix from the received TSI and then transmitting an optimized waveform. The TSI covariance is not stationary as a result of Doppler associated with the receiver and interference source; consequently, the advantage from using the optimized waveform decays with time.

The analysis was carried out using ISL's SCATS model [14-16] to characterize the TSI in terms of power, delay, and Doppler spread of the scattered signals. The scenario for this analysis includes a UHF interference source at 7,400 m altitude flying due north at a speed of 165 m/s over WSMR, NM. The

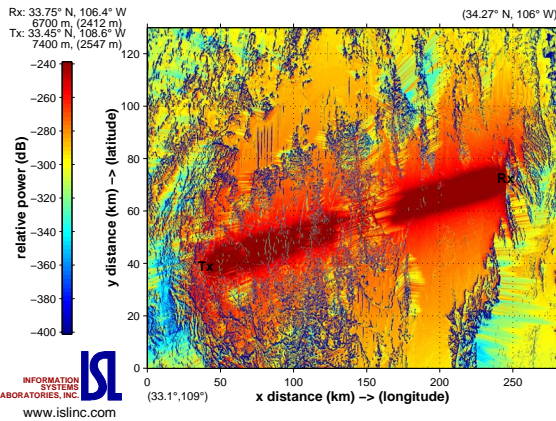


Fig. 8. Terrain scatter power calculated using SCATS.

radar is flying due north at a speed of 125 m/s 207 km to the northeast of the interference source. The interference (Tx) and radar (Rx) locations are shown in Figure 8. A white noise interference signal of 1 MHz bandwidth is assumed matched to the radar bandwidth of 1 MHz. As a result, this represents a stressing case for which there is no 'empty' portion of the spectrum for the waveform to fill.

SCATS calculates the scatter power from each scattering cell on the terrain. For this analysis a random phase chosen uniformly from the interval $[0, 2\pi]$ was assigned to each cell since the path length differences among the individual scattering elements that make up the cell span many RF wavelengths. The scattered signal from each terrain cell is then a complex number whose magnitude is the square root of the power received from the cell and whose phase is the assigned random phase modified by the propagation delay of the bistatic path. Methods of calculating the TSI covariance can be found in [10, 11]

Analysis was performed by optimizing the waveform based on the interference covariance observed on a relatively

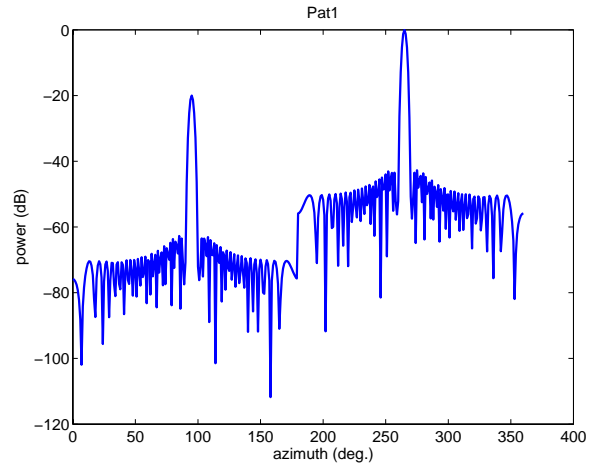


Fig. 9. Receive antenna pattern at 0 degrees elevation.

narrow spatial receive beam. For this example, the antenna is a horizontal array of 50 dipoles spaced at half wavelength. Bore-sight of the array is at 270° azimuth. The bearing to the interference source is 261° azimuth or 9° from boresight. The beam is steered to 265°, which is just 4° in azimuth from the interference. All angles are in true azimuth. The beam pattern is shown in Figure 9. A suppression of the backlobe by 20 dB can be observed in the pattern.

Gain of the optimized waveform relative to an LFM is shown in Figure 10. Here the direct path is assumed to be spatially suppressed and the coloring of the spectrum due to the interference multipath allows for some gains when using an optimized waveform. However, the non-stationarity of the interference due to the platform-motion induced Doppler shifts results in degradation with time. The waveform synthesized from 50 eigenvectors has decayed to 4 dB after 20 ms. We would expect results to vary with scenario and varying platform speeds, etc.

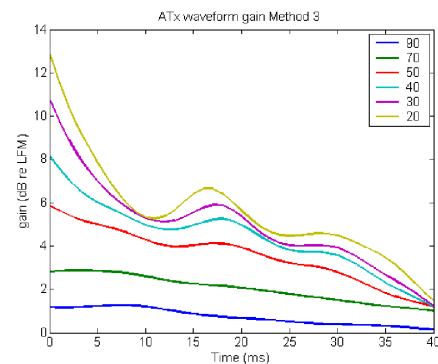


Fig. 10. Gain of using an optimized waveform synthesized at time 0 as a function of time parametric in the number of eigenvalues spanned by the optimized waveform for the steered beam (Method 3). The interference covariance was characterized using 100 lags.

5.0 SUMMARY AND FUTURE WORK

The radar waveform can be optimized to improve the system SINR performance by taking advantage of spectrum that is not occupied by the interference. Issues involve a trade-off among SINR improvement, radar detection (range resolution and sidelobes), deviation of the waveform from constant modulus, additional computational requirements, and persistence of the improvement over time until the waveform is recalculated. Even a few dB of additional interference suppression can have a substantial impact on radar performance allowing greater range, reduced power, faster surveillance revisit rates, or reduced 'burn through' requirements during engagements.

Simulations show that in the presence of partial band interference an optimized waveform can achieve substantial gains (order of 30 dB) relative to a conventional LFM waveform. The gains and quality of the resulting waveform are a function of the relative bandwidths of the interference and radar receiver.

TSI simulations showed that terrain scatter colors the interference signal spectrum. For the site-specific scenario simulated, gains in excess of 20 dB signal-to-interference ratio can be calculated but at the expense of desirable properties of the radar waveform. When the waveform is constrained to behave more like a conventional LFM waveform, the improvements are on the order of 5-6 dB. Platform-motion-induced nonstationarity of the interference results in a reduction in performance with time relative to the covariance estimate.

It was generally found that constraints are necessary on the optimized waveform to provide usable radar performance. Forcing the optimized waveform to look more like a radar waveform with desirable characteristics, e.g. LFM, improved the compressed pulse resolution and sidelobes greatly. There is a trade-off between the signal to interference improvement and the 'quality' of the radar waveform. As the eigenvector subspace used for the optimized waveform shrinks, the optimized waveform exhibits poorer pulse compression and unsteady amplitude.

Future work will consider issues regarding the impact of the use of a whitening filter on system performance, a broader range of interference scenarios, covariance estimation issues, and other methods for constraining the waveform to have desirable characteristics.

6.0 REFERENCES

- [1] L. E. Brennan and I. S. Reed, "Theory of adaptive radar," *IEEE Transactions on Aerospace and Electronic Systems*, vol. 9, March, 1973.
- [2] L. E. Brennan, J. D. Mallet, and I. S. Reed, "Adaptive arrays in airborne MTI radar," *IEEE Transactions on Antennas and Propagation*, vol. 24, September, 1976.
- [3] J. Ward, "Space-time adaptive processing for airborne radar," Lincoln Laboratory Technical Report 1015, December, 1994.
- [4] S. U. Pillai, H. S. Oh, D. C. Youla, and J. R. Guerci, "Optimum transmit-receiver design in the presence of signal-dependent

interference and channel noise," *IEEE Transactions on Information Theory*, vol. 46, no. 2, March, 2000.

- [5] J. R. Guerci and S. U. Pillai, "Theory and application of adaptive transmission (ATx) radar," *Proceedings of the Adaptive Sensor Array Processing Workshop*, MIT Lincoln Laboratory, March 10-11, 2000.
- [6] J. R. Guerci and S. U. Pillai, "Theory and application of adaptive transmission (ATx) radar," *Proceedings of the Workshop on Adaptive Sensor Array Processing (ASAP)*, 14-15 March 2000, Lexington, MA.
- [7] J. S. Bergin and P. M. Techau, "An upper bound on the performance gain of an adaptive transmitter," ISL Technical Note ISL-TN-00-011, Vienna, VA, August, 2000.
- [8] H. L. Van Trees, *Detection, Estimation, and Modulation Theory: Part I*, John Wiley and Sons, Inc., New York, 1968.
- [9] J. R. Guerci, et al, "Constrained optimum matched illumination-reception radar," U.S. Patent 5,146,229, September 8, 1992.
- [10] P. M. Techau, J. R. Guerci, T. H. Slocumb, and L. J. Griffiths, "Performance bounds for hot and cold clutter mitigation," *IEEE Transactions on Aerospace and Electronic Systems*, vol. 35, pp. 1253-1265, October, 1999.
- [11] P. M. Techau, "Performance evaluation of hot clutter mitigation architectures using the Splatter, Clutter, and Target Signal (SCATS) Model," *Proceedings of the 3rd ARPA Mountain Top Hot Clutter Technical Interchange Meeting*, August 23-24, 1995, Rome Laboratory, Griffiss AFB, NY.
- [12] R. L. Fante, "Cancellation of specular and diffuse jammer multipath using a hybrid adaptive array," *IEEE Transactions on Aerospace and Electronic Systems*, vol. 27, September, 1991.
- [13] R. L. Fante and J. A. Torres, "Cancellation of diffuse jammer multipath by an airborne adaptive radar," *IEEE Transactions on Aerospace and Electronic Systems*, Vol. 31, April, 1995.
- [14] J. E. Don Carlos, "Clutter, spatter, and target radar signal model," ISL technical note ISL-TN-89-003, Vienna, VA, November, 1989.
- [15] J. E. Don Carlos, K. M. Murphy, and P. M. Techau, "An improved clutter, splatter, and target signal model," ISL technical note ISL-TN-91-003, Vienna, VA, May, 1991.
- [16] P. M. Techau and D. E. Barrick, "Radar phenomenology modeling and system analysis using the Splatter Clutter, and Target Signal (SCATS) model," ISL technical note ISL-TN-97-001, Vienna, VA, October, 1997.

BIOGRAPHIES AND ACKNOWLEDGEMENTS

J. S. Bergin is with Information Systems Laboratories, Inc., 37 Pemberton Rd., Nashua, NH 03063 USA; (603) 880-3159, jsb@isl-inc.com

P. M. Techau is with Information Systems Laboratories, Inc., 8130 Boone Blvd., Suite 500, Vienna, VA 22182 USA; (703) 448-1116, pmt@isl-inc.com

J. E. Don Carlos is with Information Systems Labs., Inc., 10070 Barnes Canyon Rd., San Diego, CA 92121 USA; (858) 535-9680, jdc@isilinc.com

J. R. Guerci is with the DARPA Special Projects Office, 3701 North Fairfax Dr., Arlington, VA 22203 USA; (703) 248-1511, jguerci@darpa.mil